A Flexible and Robust Modelling Framework for Multi-Stream Heat Exchangers

Geir Skaugen[a](corresponding author), Kjell Kolsaker[b], Harald Taxt Walnum[a], Øivind Wilhelmsen[a]

[a] *Sintef Energy Research,Kolbjørn Hejes veg 1A, N-7465Trondheim, Norway, email: Geir.Skaugen@sintef.no, Harald.Taxt.Walnum@sintef.no, Oivind.Wilhelmsen@sintef.no*

[b] *Norweigan University of Science and Technology, Trondheim, Norway, email: kjell.kolsaker@ntnu.no*

corresponding author phone/fax: +47 73 59 39 48/+47 73 59 27 50

Abstract

Heat exchangers are important units in most industrial processes. They involve physical phenomena such as condensation and evaporation including several boiling regimes. Different types of heat exchangers constructed for different applications may differ much in geometrical design. This work explains and demonstrates a modelling framework which is capable of handling a multitude of geometries and relevant physical phenomena affecting the performance of the heat exchangers. The data structure and governing equations are explained, before the framework is demonstrated for a particular challenging test case with a heat exchanger operating similar to the main heat exchanger in a single mixed refrigerant cycle. In the test case, both evaporation and condensation may happen simultaneously along the length of the heat exchanger. 1000 cases with random changes within predefined intervals in inlet temperatures, mass flows and pressures were used to test the robustness of the model framework. The solution scheme converged in 98.7% of the cases, and in the non-converging cases, the operating conditions exceeded the physical limits of the heat exchanger. The framework demonstrated may thus be used to create flexible and robust heat exchanger models for use in process simulations, optimization, or as a stand-alone model.

Keywords: Heat exchanger, Modelling, Multi-Stream[1]

[1] **Abbreviations**

MRHP Mixed refrigerant, High Pressure
MRLP Mixed refrigerant, Low Pressure
NG Natural Gas

This is the accepted version of an article published in Computers and Chemical Engineering
http://dx.doi.org/10.1016/j.compchemeng.2012.10.006

1. **Introduction**

When process simulations and optimisation of complex processes are performed, heat exchanger equipment is often treated in a simplified manner using composite streams, constant heat transfer rates, heat capacities, and a constant or simplified pressure drop model. A typical assumption in process modelling is treating the heat exchanger as a black-box which provides the duty and the performance required by the process simulator.

A motivation for the heat exchanger modelling framework described in this paper is the need to design robust heat exchanger models which may be used as stand-alone heat exchanger design tools, or integrated as part of a simulation or optimisation flow-sheeting programs. Heat exchanger geometries will affect the system performance and with a heat exchanger model which takes this into account more realistic constraints in terms of size and operability can be provided when performing system analysis. Skaugen et al. (Skaugen et al. 2010) showed that a heat exchanger designed for a maximum process efficiency may suffer to static instabilities. These static instabilities may be avoided by changing to less efficient operating conditions or alter the heat exchanger geometry. A modelling framework with sufficient level of geometry details is necessary to take these effects into account. Heat exchangers using several parallel channels with complex heat transfer interactions between streams like brazed aluminium plate-fin heat exchangers are a typical example of a challenging heat exchanger to model with respect to this.

Modelling of multi-stream heat exchangers is a mature research subject, and analytical expressions have been developed for simplified heat exchanger models by for instance Chato (1971). A common approach in simulations of heat exchangers in the 1960-70's and also later, was to use constant heat capacities and heat transfer rates, which resulted in a system of equations with the local fluid temperature as the only unknown variables. Pressure drop was seldom included and phase change with constant temperature over a certain length of the heat exchanger was treated separately.

Paffenbarger (1990) describes a steady state rating program, MSE, that was developed after a review of available articles on aspects relevant for multi-stream heat exchangers, like the effect of axial heat conduction, heat exchange with the environment, mal-distribution of flow. He concluded that an acceptable cryogenic multi-stream heat exchanger model should take into account: Variable physical properties, axial heat conduction within the metal and, for a plate-fin in particular, layer order and cross-layer conduction through fins. In his model he uses local stream temperatures, stream pressures and wall temperature as the set of unknown variables along the stream path for each channel. Only single component and single-phase fluid was implemented in the model and solved via a simultaneous solution approach. He demonstrated the tool by evaluating the effects of different layer configuration and the effect axial heat conduction for a three-stream plate-fin heat exchanger. In this model the effect of including axial heat conduction accounted for 15% additional surface area to get the same heat exchanger efficiency as the similar case excluding this effect.

Prasad (1997) used almost the same equations as Paffenbarger (1990) in his computer program called STACK, but the governing equations are integrated over the entire length of the heat exchanger and in an outer iterative loop all unknown fluid and surface temperature are compared to the values from the previous iterations. An iterative outer loop was chosen both to reduce the problem size and to get more control with the local variables.

Pingaud et.al (1989) proposed a generalized method for steady-state and dynamic simulations of plate-fin heat exchangers based on state of the art physical and thermodynamic models. They included non linear heat-transfer, frictional pressure drop, phase slip using real thermodynamic and transport properties. Their model decoupled the fluid properties from the metal or partition sheet temperatures. The hydrodynamic equations of each fluid channel were solved successively by integration, with known metal temperatures, and as the next step, the thermal balance for the metal temperatures were solved using sparse matrix techniques. Corberan et al (2001) proposed to call this technique for WTLE (Wall Temperature Linked Equations). The specific enthalpy, pressure and the metal temperature are the variables used by Pingaud et.al. (1989).

At SINTEF, several heat exchanger models have been developed in the past and used to design laboratory off-the shelf prototypes (Pettersen et al. 1998; Skaugen 2000) and used in process evaluation, simulation and optimization (Fredheim et al. 2000; Skaugen 2003; Skaugen et al. 2010) These models are often based on laboratory validated sub-models (Neeraas et al. 2004). Noticing that heat exchanger models often exhibit similar properties, the motivation for developing a new modelling framework is to be able to consistently develop models representing different types of heat exchangers with less effort. It should be possible to investigate both established and novel concepts with the framework. For a multi-stream heat exchanger model the framework should be able to handle the following challenges:

This is the accepted version of an article published in Computers and Chemical Engineering
http://dx.doi.org/10.1016/j.compchemeng.2012.10.006

- Detailed heat exchanger geometries
- Local metal temperatures included in the calculations
- Individual stream approach
- Conductive heat transfer in the metal, convective heat transfer in the fluid and radiant heat transfer between metal-surfaces.
- Modular design for selection of models for:
    - Heat transfer and pressure drop
    - Numerical methods
    - Thermodynamic and transport property
- Effect of flow mal-distribution (sensitivity)

The modelling framework described in the Sections 2 and 3 is geometrically generic and can be used to describe a variety of heat exchanger types and configurations. The framework is designed to use any thermodynamic library if the necessary thermo-physical properties are available. A robust solution scheme and state of the art heat transfer coefficient and pressure drop correlations have been implemented. In Section 4 a multi-stream, multi-component heat exchanger for liquefaction of natural gas where phase change occurs in all streams has been modelled and tested for robustness. Conclusions will be given in Section 5.

2. **Description of the modelling framework**

2.1. The computer structure of the modelling framework

Modelling of heat exchangers is challenging when the geometry becomes complex. To avoid the necessity of using a complete 3D geometric model and a full CFD simulation, a set of building blocks has been developed. The building blocks are simplified, yet complete enough to represent the most common geometries found in heat exchangers. They can be viewed as basic unit operations with one or more interfaces that allow connection following specific rules. The framework has been implemented in the programming language C using an object-oriented approach.

The main idea is to use basic geometrical aspects of pipe flow without the need of a fully general 3D model. Instead a parameterization is applied to create both a non-geometrical mathematical model and a geometrical model that serves as visualization.

A good example is the fluid element (FHXElement). It contains a model for pipe or channel flow with heat exchange to the surrounding surfaces. The generalized geometry for the fluid element is represented by a length, a circumference and a cross section area. Other quantities can be derived from these data, e.g. the hydraulic diameter. This is a useful observation when operating with one-dimensional (1D) fluid flow and simplifies the creation of models even for complex geometries. The 1D restriction can be lifted by extending the parameters for the fluid element. The fluid state for an element is provided by the FHXNode that stores local values of all the thermodynamic and transport properties needed for calculations of local heat transfer and pressure drop.

The basic building blocks can be grouped into several categories, encapsulating the different parts of the total simulation. The building blocks shown here represent the physical framework needed to set up the complete equation set. Yet other components not shown here handle the selection of solution method, calling the appropriate solver(s), input-output and so on. They integrate closely with the presented framework.

Table 1 Overview of some key-components in the heat exchanger framework

	Category	Components	Interfaces
0	Heat exchanger model	FHXModel	The owner of all components listed below in 1-8
1	Thermal conduction	FHXSolidNode, FHXThermalBridge	FHXSurface, and internally (electric analogy)
2	Surface	FHXSurf	FHXThermalBridge, FHXElement
3	Fluid flow	FHXElement	FHXSurf, and upstream

This is the accepted version of an article published in Computers and Chemical Engineering
http://dx.doi.org/10.1016/j.compchemeng.2012.10.006

		FHXJunction	
4	Thermodynamic equilibrium	FHXNode	FHXElement, FHXPhys
5	Link to external libraries for thermodynamics and material data	FHXPhys FHXMaterial FHXInsulation	FHXNode, FSolidNode, FSolidBridge
6	Macro models	FHXBundle FHXCube FHXPlate	Automatically creates valid networks of the above components
7	Helper models	FHXPass FHXBundleTube FHXPlateTube FHXLayer FHXGeometry	Data structures aiding the setup of equations and access of data
8	Simplified models	FHXElementSimplifiedData, FHXSurfSimplifiedData	Available to the solver during e. g. initialization.

One class of components (category 1, 2, 3, 4 and 5) provides the physical building blocks. These components isolate the different physical processes that occur in heat transfer:

- Thermal conduction (category 1) is represented by a thermal heat capacity node and a thermal resistor. In principle, any geometry can be represented by an electric analogy, but the elements are best suited for simple 1D heat transfer across two sides, possibly supplied with longitudinal heat transfer (quasi 2D).
- A surface element (category 2). This element serves as a connection between the fluid and the solid, and provides a link to the relevant heat transfer correlations.
- Fluid flow elements (category 3), represent a 1D node for fluid flow along a channel. It contains the pressure drop calculation and serves as a connection to one or more surface elements, and the upstream fluid element. The junction element does merging and splitting of streams, and is rarely needed in the basic configurations, therefore not seen in the collaboration diagram in Figure 1
- A thermodynamic element (category 4) of the fluid represents the connection to the thermodynamic properties of the fluid, and is isolated from the fluid flow element. The thermodynamic element handles single or multiple phases, and serves as an abstract interface to an external thermodynamic library.
- Link to physical data other than thermodynamics are summarized in category 5.

A different class of components (category 6) is a set of parameterized macro blocks. They handle the connection of basic building blocks. One example is the model called FHXBundle in Figure 1, allowing a wide variety of geometries, even tubes inside tubes. These include coaxial heat exchangers, tubes-in-shell geometries, and multi-stream LNG heat exchangers with spiral wound tubes. In theory there can be tubes inside tubes inside tubes, although these geometries are rare. The macro provides an interface to create the complete system from the basic building blocks. It handles the definition of all the involved components, doing the connections, and calculating the individual parameters of each component.

Different parameterized macro blocks can define different geometries, such as a plate-heat exchanger or a plate-fin heat exchanger. A parameterized version of a complex heat exchanger can thus be used as a unit model in an engineering flow sheeting environment or as a dynamic link library in a spreadsheet program like Microsoft Excel. The parameterized macro needs very little geometry input and may easily be part of a larger heat exchanger/process optimization for instance as outlined by Reneaume and Niclout (2003) They defined a number of geometric parameters subjected for optimization like fin geometry, core width and so on for a plate-fin heat exchanger using various mathematical approaches, and a fully detailed heat exchanger model, when evaluating the object function.

This is the accepted version of an article published in Computers and Chemical Engineering
http://dx.doi.org/10.1016/j.compchemeng.2012.10.006

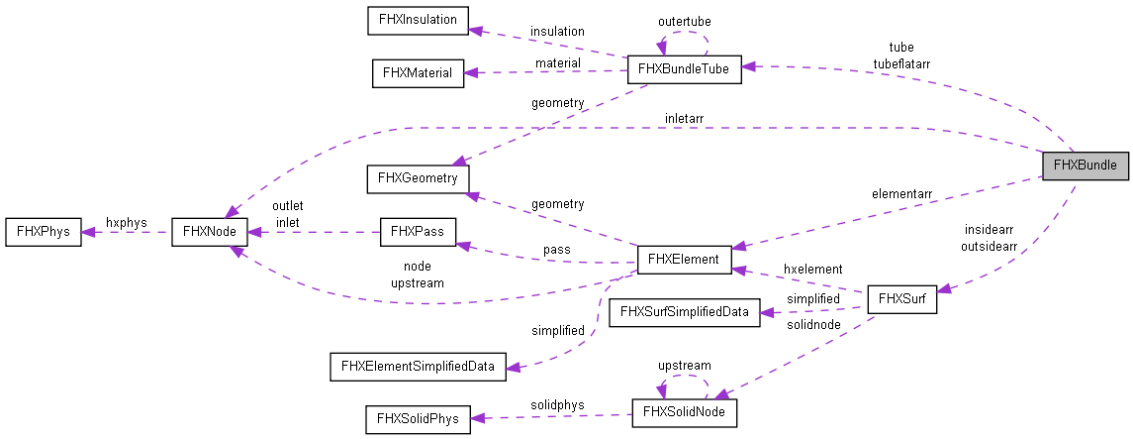

Figure 1 Collaboration graph for the FHXBundle macro-block

The macro has an interesting aspect that it can also be used to create a complete geometric 3D model of the heat exchanger from the parameterized input. This functionality may be used to visualize the heat exchanger in 3D using e.g. VTK (Schroeder et al. 2006) or export to a CAD model. The 3D model can also be used to calculate the weight of the construction, and it can be used to check that the desired geometry really exists without undesired collisions in space. Another use of the 3D model is data visualization for result presentations.

Category 7 and 8 in Table 1 contain some helper components. In a simulation, there is one single system, or model, treated as a singleton. The system sets up the equation system, and provides hooks to a varying set of solvers and solution methods. An algorithm built into the system automatically creates the passes from the information given in the fluid flow elements. When the heat exchanger is readily connected, the passes become part of a complete model representing the flow paths in the heat exchanger, completely connected to the boundary conditions. The model is solved by looping over all passes and integrating the heat transferred through the various surfaces and the pressure-state over all fluid elements in each pass. During the integration within each individual element, some integrated properties are saved in a simplified (linear) model (8) that can be used as a fast alternative when updating the metal temperatures later.

2.2. How to handle different geometries

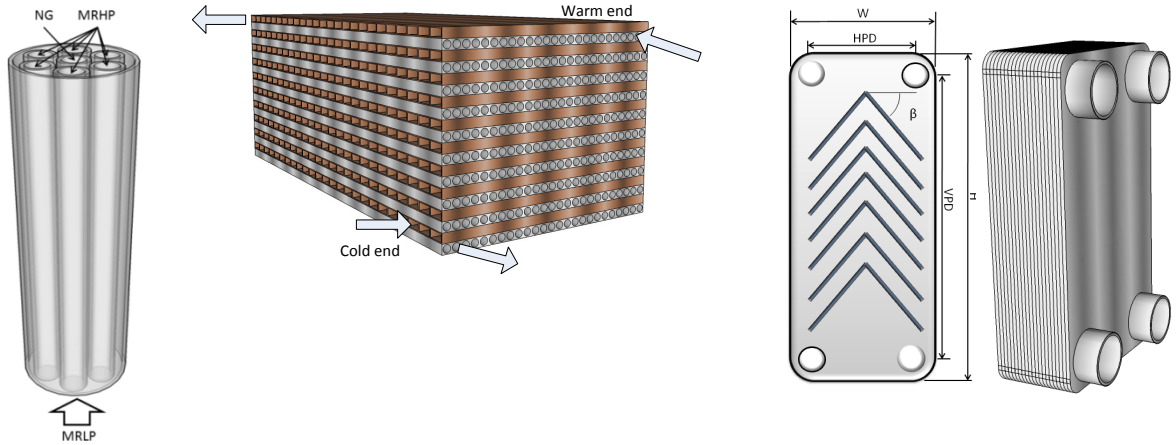

a) b) c)

Figure 2 Example of implemented common heat exchanger geometries in the modelling framework

This is the accepted version of an article published in Computers and Chemical Engineering
http://dx.doi.org/10.1016/j.compchemeng.2012.10.006

The tube-in-shell exchanger in Figure 2a, the multi-dimensional cross-stream in Figure 2b and the plate heat exchanger in Figure 2c have fundamentally different geometries. They can all be handled by the geometrically flexible modelling framework elucidated in this work. How a three-stream variant of the multi-stream tube-in-shell heat exchanger, (2a), is represented in the framework is shown in Figure 3. (The other two geometries will require a different configuration). Here the various elements like fluid elements, surfaces, heat-nodes and solid bridges are shown and numbered. As illustrated: In the data structure describing the heat exchanger, the mantle stream is linked to three surfaces, the outside wall of the two tube streams as well as the inside of the mantle wall. The (solid) heat-nodes representing the inside and outside tube wall temperatures are linked through a resistor element – a solid bridge. In this particular model, the mantle wall temperature is represented by only one heat-node for each axial calculation element. The heat balance equation for that heat-node can also include heat loss to the ambient – if specified - through an insulation layer. The insulation could have been specified as two heat nodes, a solid bridge and with the ambient as a fourth fluid node. This would increase the number of equations unnecessary. The sequence of elements shown in Figure 3 is connected through the fluid-nodes *N* number of times to form the three fluid passes. The wall elements can also be connected through additional heat nodes and solid bridges to form an actual tube wall with axial conduction resistance.

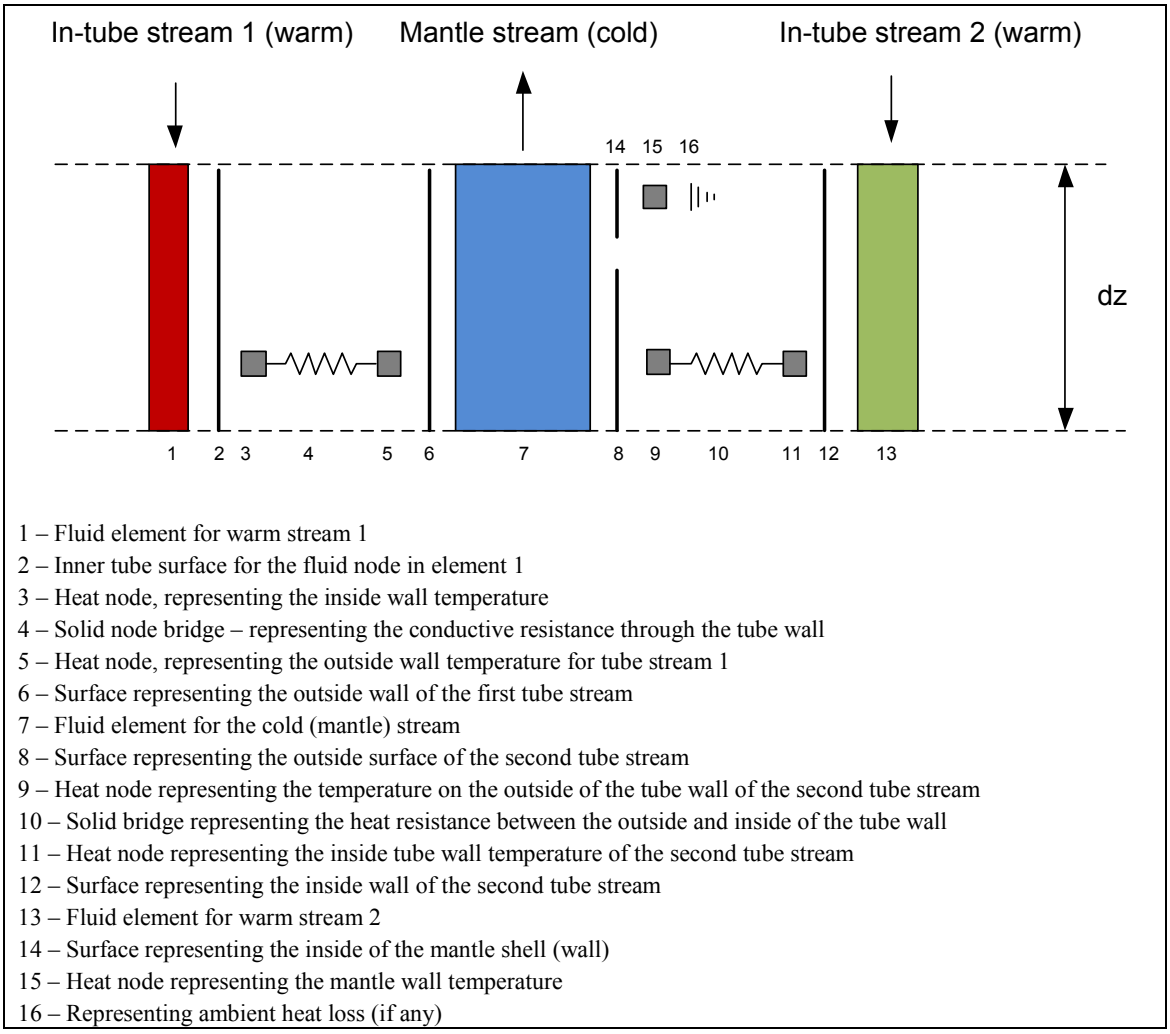

1 – Fluid element for warm stream 1
2 – Inner tube surface for the fluid node in element 1
3 – Heat node, representing the inside wall temperature
4 – Solid node bridge – representing the conductive resistance through the tube wall
5 – Heat node, representing the outside wall temperature for tube stream 1
6 – Surface representing the outside wall of the first tube stream
7 – Fluid element for the cold (mantle) stream
8 – Surface representing the outside surface of the second tube stream
9 – Heat node representing the temperature on the outside of the tube wall of the second tube stream
10 – Solid bridge representing the heat resistance between the outside and inside of the tube wall
11 – Heat node representing the inside tube wall temperature of the second tube stream
12 – Surface representing the inside wall of the second tube stream
13 – Fluid element for warm stream 2
14 – Surface representing the inside of the mantle shell (wall)
15 – Heat node representing the mantle wall temperature
16 – Representing ambient heat loss (if any)

Figure 3 A three-stream heat exchanger represented in the heat exchanger modelling framework

This is the accepted version of an article published in Computers and Chemical Engineering
http://dx.doi.org/10.1016/j.compchemeng.2012.10.006

3. **Solution method**

The solution scheme of the modelling framework alternates between solving each fluid pass with fixed metal temperatures and then solving the wall temperatures with fixed fluid pass conditions. This is similar to the "wall temperature linked equations" (WETLE) discussed by Corberàn (Corberân et al. 2001). The specific enthalpy and pressure are used as the local state variables along each fluid pass. The solution procedure follows these three steps:

1. The problem is initialized with fluid inlet properties and a wall temperature profile. The wall temperature profile is initialized as a linear profile between the cold and warm end as default.
2. The fluid elements are then solved based on the wall temperature (see chapter 3.1).
3. The wall temperatures are then updated based on the net heat fluxes over each surface coming from the fluid calculations described below.

The second and third steps are repeated until convergence is reached. Convergence is defined as the state when there is no change in any metal temperatures between two successive iterations. This has to be below a predefined convergence-criterion. As an additional check the sum of all the fluid element heat balances is performed.

3.1. Fluid calculations

As discussed previously, a fluid pass is defined as a linked sequence of fluid elements. All the fluid elements have a fixed geometry (length). The fluid calculations is thus to determine the transferred heat and pressure drop for each pass in a heat exchanger. Within each element in a pass, the specific enthalpy, the pressure drop gradient and the heat transferred though each surface is integrated. The integration may be performed either as a set of ordinary differential equations (ODE) with fixed or variable step-length or as a set of differential algebraic equations (DAE). During the integration, each fluid element surface uses the same wall temperature along the whole length of the element.

All fluid-elements are solved starting from the inlet of each pass, defined by the specific enthalpy (h) and the pressure (p). For each new h and p an enthalpy-pressure flash must be performed to determine the number of phases, the liquid and vapour compositions, temperatures and vapour fractions. With a known state, the transport properties like conductivity and viscosity for all phases can be calculated. For a DAE formulation, the fluid elements are calculated by solving the following balance equations

Specific enthalpy:

$$h = h_0 + \int_{x0}^{x0+\Delta x} \frac{\mathrm{d}h}{\mathrm{d}x}(h,p)\,\mathrm{d}x \qquad \text{Eq. 1}$$

$$\mathrm{res_h} = -\frac{\mathrm{d}h}{\mathrm{d}x}(h,p) + \frac{\sum \mathrm{d}q_i}{\dot{m}} \qquad \text{Eq. 2}$$

This is the accepted version of an article published in Computers and Chemical Engineering
http://dx.doi.org/10.1016/j.compchemeng.2012.10.006

Here, Δx is the length of the fluid element and x is the spatial direction of the flow. Eq. 1 shows the integration of total enthalpy through the energy balance of a specific stream. The specific enthalpy term contains both the enthalpy of the gas and the liquid in the two-phase area. Subscript "0" denotes the inlet conditions of the fluid element. The specific enthalpy is connected to the heat flux through the element surface as given by Eq. 2, where the residual on the left hand side should be below a predefined convergence criteria in the final solution. The heat flux $\mathrm{d}q_i$ for surface i is:

$$\mathrm{d}q_i = \frac{T_{w,i} - T_F}{R_{tot,i}} \qquad \text{Eq. 3}$$

Here, $T_{w,i}$ and T_F are the wall and fluid temperatures and $R_{tot,i}$ is the total heat transfer resistance. The heat transfer resistance is a result of convective heat transfer to the surface and fouling resistance at the surface. These contributions may be estimated using semi-empirical relations. The integrated momentum balance gives the pressure profile inside the heat exchanger:

$$p = p_0 + \int_{x0}^{x0+\Delta x} \frac{\mathrm{d}p}{\mathrm{d}x}(h,p)\,\mathrm{d}x \qquad \text{Eq. 4}$$

The pressure gradient is a sum of the frictional pressure gradient calculated by a frictional factor correlation (subscript *f*), and a gravitational pressure gradient, (subscript *g*) calculated as $\rho_{tp}g$ with a void fraction correlation to get a two-phase density ρ_{tp} and g as the gravitational constant. With a horizontal heat exchanger, the gravitational contribution is zero.

$$\mathrm{res_p} = -\frac{\mathrm{d}p}{\mathrm{d}x}(h,p) + \left[\left(\frac{\mathrm{d}p}{\mathrm{d}x}\right)_f + \left(\frac{\mathrm{d}p}{\mathrm{d}x}\right)_g\right] \qquad \text{Eq. 5}$$

The heat flow through each surface, *i,* is also obtained in the integration:

$$q_i = \int_{x0}^{x0+\Delta x} \frac{\mathrm{d}q_i}{\mathrm{d}x}(h,p)\,\mathrm{d}x \qquad \text{Eq. 6}$$

This gives the following residual which should be below a predefined convergence criteria in the final solution:

$$\mathbf{res}_\mathrm{q} = -\frac{\mathrm{d}q_i}{\mathrm{d}x}(h,p) + \mathrm{d}q_i \qquad \text{Eq. 7}$$

The term dq_i/dx ([W/m]) is calculated from the local heat transfer resistance, R_i,$[m^2K/W]$ between the surface and fluid temperature as:

$$\frac{\mathrm{d}q_i}{\mathrm{d}x}(h,p) = \frac{T_{w,i} - T_{F,i}}{R_i} \cdot S_i \qquad \text{Eq. 8}$$

S_i [m] is the perimeter for the surface (the heat transfer surface per. length). The fluid temperature $T_{F.i}$ [K] is calculated from a thermodynamic enthalpy-pressure flash and the heat transfer resistance is calculated using an appropriate empirical correlation for the heat transfer coefficient, depending on whether the stream is heated, evaporated, cooled or condensed. Notice that the formulation above differs from some heat exchanger models where a complete fluid *stream* has a corresponding energy and momentum equation. In this work, an energy and

This is the accepted version of an article published in Computers and Chemical Engineering
http://dx.doi.org/10.1016/j.compchemeng.2012.10.006

momentum balance should be satisfied for each fluid element. The advantage of this approach is that the model is flexible, in that a fluid stream may interact with different fluid streams at different geometrical locations. The number of interactions between the fluid streams is only limited by the number of fluid-elements, and the available interaction perimeter.

Three different differential equation solvers have been tested for solution of the fluid elements: DASSL, as a DAE formulation, and Runge-Kutta-Fehlberg (RKF) from the SLATEC library (SLATEC 1993) and an in-house implementation of a classical fourth order explicit Runge-Kutta formulation (RK4). The SLATEC solvers are efficient and accurate; however, the implementation of the RK4 yields better control of the solution routine in terms of local fluid properties and step length. The heat transfer coefficient (HTC) and frictional and gravitational pressure gradients are calculated with appropriate correlations for the particular fluid/surface interface. After the integration of one fluid element has finished, the values on the boundary are used as input to the next element.

3.2. Wall temperature update

The wall temperature update strategy is to set up a system of equations for each solid-node in the model based on the heat fluxes for each surface calculated from the fluid pass integration and conductive heat transfer over the solid-bridges. The equation system is solved using the general non-linear solver DNSQE in the SLATEC library. This uses a modified hybrid Powel method (Powel 1988). In this formulation, the solid-node temperatures are considered the unknown variables to be found. There is one residual function g_i for each solid-node in the model shown as Eq. 9. Each residual has to be below the convergence criteria in the final solution.

$$g_i = \sum_{j=1}^{NS(i)} q_{\text{conv}} + \sum_{k=1}^{NSB(i)} q_{\text{cond}} \qquad \text{Eq. 9}$$

The first term is the sum of the convective heat fluxes through each surface linked to the solid-node, *i*. The number of surfaces seen by each solid-node is *NS(i)*. The convective heat fluxes for each surface element is stored during the integration of each fluid pass as outlined above. The solid-bridges account for the heat conduction in all directions, within the wall, q_{cond}. The total number or solid-bridges as seen from the solid-node is *NSB(i)*. In addition, a radiant term may be included if radiation is an important heat transfer mechanism. The conductive heat flux is defined as:

$$q_{\text{cond}} = \frac{T_{s,\text{otherside}} - T_s}{R_{\text{sb}}} \qquad \text{Eq. 10}$$

$T_{s,\text{otherside}}$ is the (heat-node) temperature on the solid-node on the "other side" of a solid-bridge. This is a pointer set up during the generation of the model. T_s is the wall temperature and R_{sb} is the conductive resistance term for the solid-bridge, which could be either axial or radial.

4. **Demonstration of the modelling framework**

In the next sections, the robustness of the solution scheme outlined in the previous section will be discussed.

4.1. Description of the test case

It is challenging to capture all relevant physical mechanisms in heat exchangers found in the LNG industry. A heat exchanger model operating similar to the main heat exchanger in a single mixed refrigerant cycle has thus been chosen to test the robustness of the modelling framework and the solution schemes used.

Geometrically, the model is designed as a multi stream tube and shell heat exchanger with the natural gas (NG) and the hot high pressure mixed refrigerant (MRHP) entering the tubes at the top of the heat exchanger, and the cold low pressure mixed refrigerant (MRLP) entering the shell side at the bottom. Temperatures, pressures, compositions and flow rates at the inlet are the same as used by Skaugen et al.. 1.0 kmole/s of natural gas is cooled, condensed and subcooled from superheated conditions 298 K at 55 bar by evaporating 3.15 kmole/s of mixed hydrocarbon

This is the accepted version of an article published in Computers and Chemical Engineering
http://dx.doi.org/10.1016/j.compchemeng.2012.10.006

refrigerant at 5 bar and 116.05 K. The refrigerant is also used to condense and subcool the refrigerant itself from 298 K and 25.8 bar. For the three streams, heat is transferred both in single phase, gas and liquid, and in the two-phase region as both evaporation and condensation.

The correlations for frictional pressure drop and heat transfer coefficients used in the demonstration case are listed in Table 2.

Table 2 List of correlations used for the demonstration case

	Single phase	Two phase
Pressure drop	An explicit Colbroook/White formulation by Selander (Selander 1978)	Friedel (Friedel 1979) – with the single phase formulation by Selander
Heat transfer	Gnielinski (Gnielinski 1976)	Boyko and Kruhzilin (condensation) (Boyko and Kruzhilin 1967)
		Bennet and Chen (evaporation) (Bennett and Chen 1980) Using the Forster-Zuber(Forster and Zuber 1955) correlation for the nucleate boiling term
		Silver, (Silver 1947) and Bell and Ghaly (Bell and Ghaly 1973) for correction of the mixture effects in multi-component condensation and evaporation

Challenges arise when the details of local heat transfer and pressure drop are resolved. When a fixed grid is used for the metal wall elements, the location of the phase changes may change between iterations with discontinuities affecting the solution algorithm. To have a more robust model, both the heat transfer coefficient and the pressure drop gradient should have a smooth transition between the two-phase and the single phase regions. For the evaporating streams, there is also a transition in regimes where nucleate boiling occurs. Whether nucleate boiling occurs depends heavily of the local heat flux (and consequently the wall temperature). This phenomenon is thus directly coupled to the outer iteration loop with the determination of the wall temperatures, and can have a significant effect on the local heat transfer and affect the convergence when integrating the process streams from inlet to outlet. In the Forster-Zuber equation used for nucleate boiling, both the temperature difference between the bulk stream and the wall and the difference of that bulk and wall saturation pressure are multiplied. If the initial, or calculated, wall temperatures differs too much from the stream temperature, these terms can be very large and provoke calculation and convergence challenges.

The Forster-Zuber equation for nucleate boiling:

$$a_{nb} = 0.00122\left[\frac{k_l^{0.79} c_{p,l}^{0.45} \rho_l^{0.49}}{\sigma^{0.5} \mu_l^{0.29} h_{\mathrm{lg}}^{0.24} \rho_g^{0.24}}\right]\left(T_w - T_{\mathrm{sat}}\right)^{0.24} \Delta p_{\mathrm{sat}}^{0.75} \qquad \text{Eq. 11}$$

Δp_{sat} is the difference between the saturation vapour pressure at the wall temperature and the fluid temperature.

The pressure difference is in [Pa] so a large temperature difference between bulk and wall will have a large effect on this term. In the code a restriction on the temperature difference of 4K with a corresponding pressure difference during the initial calculations of the heat transfer rates for a fluid stream.

4.1.1. Simulation results

Results from the simulations are shown in Figure 4. The left illustration in Figure 4 shows the stream temperatures. The mantle stream is heated, starting at the outlet (1.0) and ending up at the inlet (0). The two tube streams flowing in the opposite direction are cooled. In the illustration to the right, the corresponding vapour fraction profiles are shown. The natural gas (NG) enters as superheated vapour and is de-superheated in the first 40% of the heat exchanger, condensed during the next 20% and finally sub-cooled during the remaining 40%. The second tube stream is the high pressure mixed refrigerant (MRHP), entering in the two-phase region with a vapour

This is the accepted version of an article published in Computers and Chemical Engineering
http://dx.doi.org/10.1016/j.compchemeng.2012.10.006

fraction of about 0.65, and then being fully condensed during the first 80% of the heat exchanger and finally sub-cooled in the remaining 20%. The low pressure mixed refrigerant (MRLP) enters the heat exchanger at the cold end (1.0) with a vapour fraction of about 0.08 and leaves slightly superheated. The individual wall temperatures are shown, but it can be noted that due to large variations in local heat transfer coefficients and specific heat capacities along the heat exchanger, the temperatures of the two warm streams can cross. (but never with the cold stream). This happens twice in this example. The natural gas and the high pressure mixed refrigerant condensate with a large temperature glide, so at high vapour fractions the heat transfer coefficient can be severely degraded due to the added resistance of cooling the vapour phase. This shows the significance of not using a "common wall temperature"- or a "common hot stream temperature"- approach in a multi-stream heat exchanger model

With condensation and evaporation happening simultaneously in the heat exchanger large changes in heat transfer rate and pressure drop are expected It is clear that solving this heat exchanger with varying operation conditions requires a robust model and solution scheme, able to handle highly non-linear equation systems describing several phase-changes.

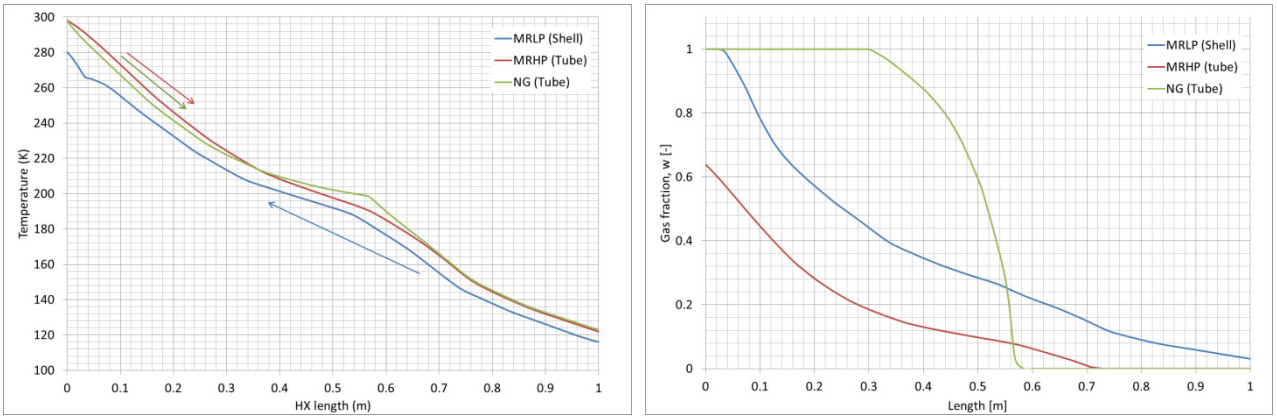

Figure 4 Temperature and corresponding vapour fraction profile for one test case

The solution scheme discussed previously enables a high accuracy in the overall heat balance. In addition, it is important to perform a grid density check, to reveal the sufficient amount of fluid and wall elements necessary to achieve a consistent solution. The number of elements will have a large impact on the computational time, and the optimal number of fluid and wall elements will be a trade-off between accuracy and speed. Figure 5 shows how simulations with the base case approach the same solution when the number of wall elements is increased. The figure shows the relative deviation in the heat transferred to the shell side, compared to a solution with 500 elements. It is evident that the solution approaches the high resolution case fast, and the sufficient number of wall elements depends on the predefined convergence criteria. New cases will need a new evaluation of the grid density.

This is the accepted version of an article published in Computers and Chemical Engineering
http://dx.doi.org/10.1016/j.compchemeng.2012.10.006

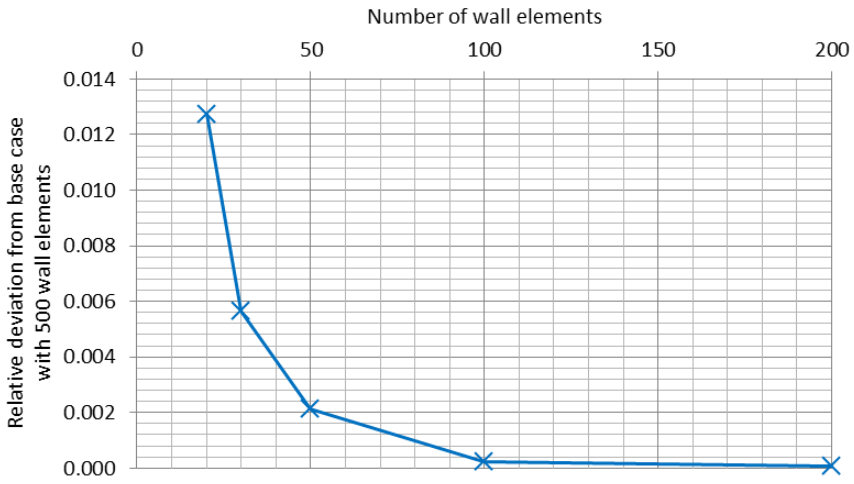

Figure 5: Solution convergence with increasing number of elements

This is the accepted version of an article published in Computers and Chemical Engineering
http://dx.doi.org/10.1016/j.compchemeng.2012.10.006

4.1.2. Test of robustness

To test the robustness of the model and the solution strategies, 1000 cases were generated by changing the operating conditions randomly within pre described ranges around the operating conditions of the base case (Skaugen et al.). Geometry and compositions were held constant, but the other inlet operating conditions were varied randomly within the ranges in Table 3.

Table 3 Range of operating conditions for validation purposes

	Range	**Nominal condition**
Inlet cold refrigerant temperature (K)	100 – 150	116.05
Inlet temperature difference (hot-cold) (K)	10 – 150	182.1
Inlet cold refrigerant pressure (bar)	2 – 10	5.0
Inlet warm refrigerant pressure (bar)	12 – 50	28.5
Inlet NG pressure (bar)	30 – 70	55.0
Flow rate MR LP (kmole/s)	0.1575 – 6.30	3.15
Flow rate MR HP (kmole/s)	0.1575 – 6.30	3.15
Flow rate NG (kmole/s)	0.05 – 2.0	1.0

These operating ranges cover the expected range of operating condition encountered in process optimisation of the single mixed refrigerant cycle. (The flow-rate ranges are varied from 5 to 200% of the nominal flow-rate.) The 1000 randomly generated operating conditions lead to heat exchanger simulations which have very different behaviour. In a case with a very small temperature gradient, T_{in} warm will be very close to T_{in} MRLP in Figure 6. The heat exchanger will operate at pinch conditions for the whole length with moderate heat transferred. With large temperatures gradients and flow rates, the heat exchange may be very high. Boiling and condensation may proceed violently in small sections of the heat exchanger, which poses a challenge for any heat exchanger model. The scattered distribution of inlet conditions in Figure 6 indicates that the robustness of the heat exchanger model is well tested for the single mixed refrigerant cycle. Similar graphs can be shown also for the other inlet condition parameters from Table 3.

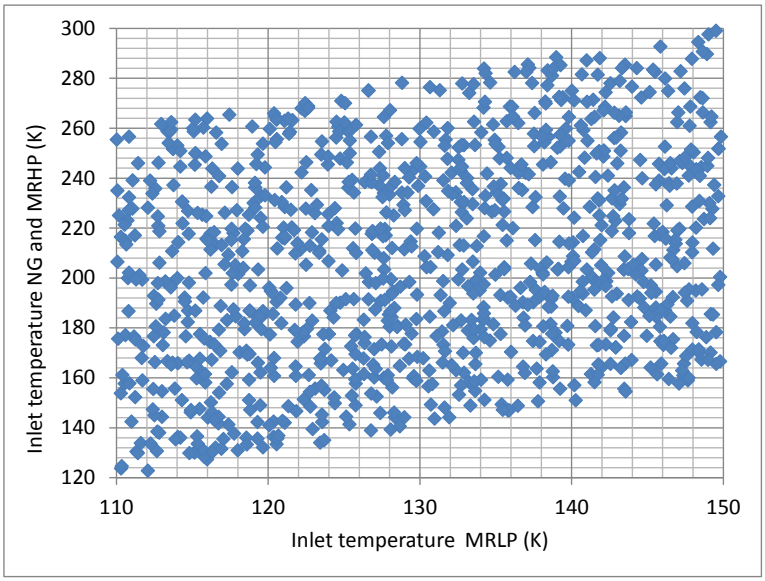

Figure 6 Variations in the inlet temperatures of the hot and cold side in the robustness test

Examples of cases resulting from the robustness test are shown in Figure 7 as a set of temperature profiles. With flow rates from a feasible industrial case, the temperature differences will vary little through the heat exchanger, (Figure 7a). This might be a case which performs well from an energy efficient point of view also discussed with respect to optimisation in (Skaugen et al. 2010). With small differences in the inlet temperatures at the hot and cold

This is the accepted version of an article published in Computers and Chemical Engineering
http://dx.doi.org/10.1016/j.compchemeng.2012.10.006

side, the local temperature difference will be small and the heat exchanger will be close to pinch over the whole length (Figure 7b).

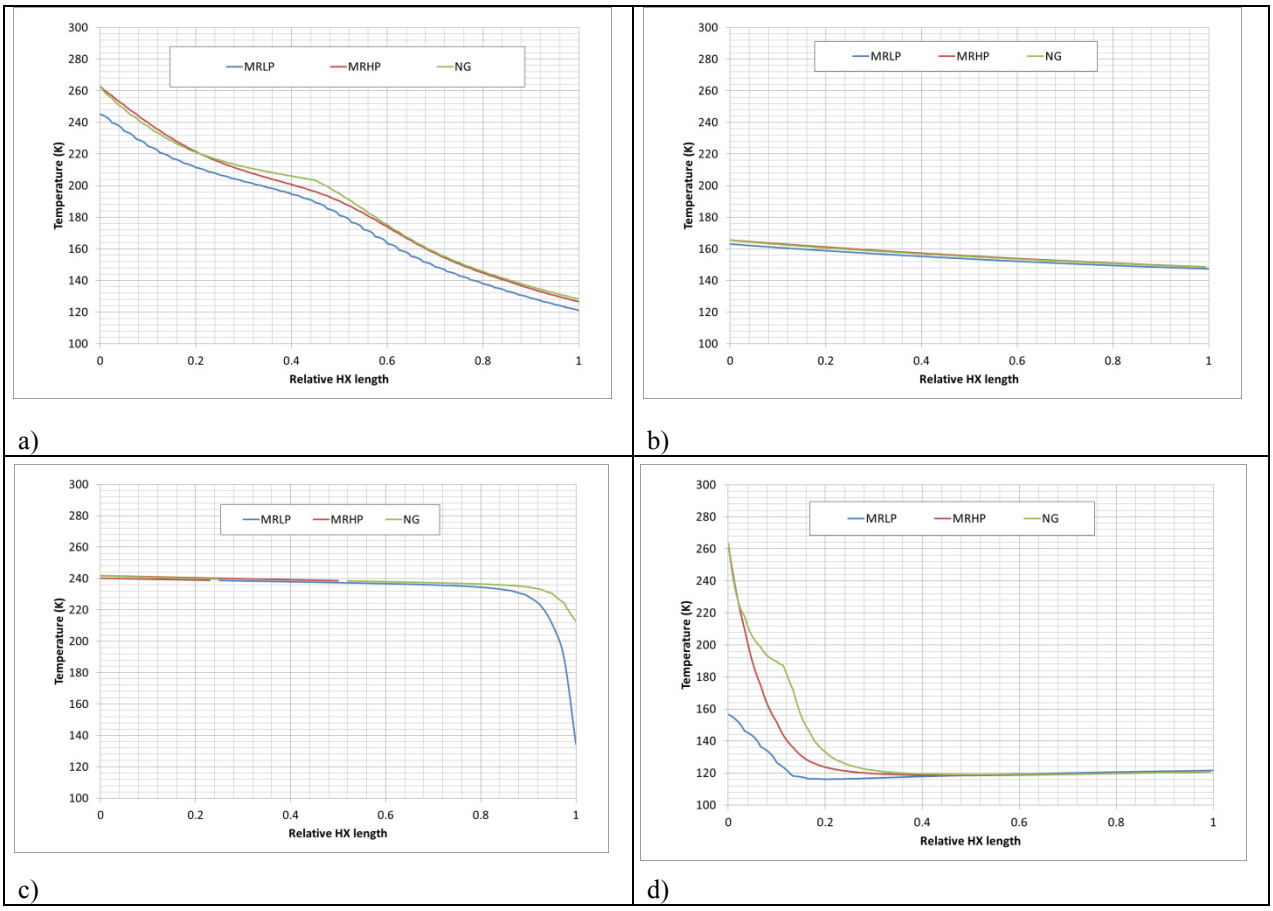

Figure 7 Results from heat exchanger simulations

This is the accepted version of an article published in Computers and Chemical Engineering
http://dx.doi.org/10.1016/j.compchemeng.2012.10.006

This is a challenging simulation due to the close to identical stream temperatures at each axial position in the heat exchanger. With differences in the flow rates, and thus also heat capacities of the streams, situations may arise where most of the heat is transferred in the cold end (Figure 7c) or in the warm end of the heat exchanger (Figure 7d). In this case it can be noted that the shell side flow rate is considerable, resulting in a temperature decrease due to a large pressure drop. Even with the large range of inlet conditions from Table 3, the solution scheme described in previous sections converged successfully in 98.7% of the cases. The cases which did not converge were examined in detail. In flow sheet calculations, the mass flow will be an input to the heat exchanger model. In the robustness test, some mass flows were too large, which resulted in very high pressure gradients and a pressure profiles falling below 0 Pa. These simulations are unphysical, meaning that the mass flow is too large for steady-state flow through a fully geometrically specified heat exchanger at these inlet conditions. Similar effects could be observed on the specific enthalpy integrating to a value below a thermodynamic lower limit. To handle these situations, two exponential function forms were developed. One for the pressure profile and one for the specific enthalpy profile. They are defined to asymptotically approach minimum values at the end of a fluid pass. These functions do not have calls to thermo physical properties, but provide the integrator with a value that can used to calculate the necessary heat balances. When an unphysical local condition is encountered during integration, the calculation of this pass is restarted using the mathematical expressions. The solid temperatures are updated as described in Section 3, and the integration is restarted with updated surface temperatures. If unphysical conditions are still found after the final iteration, the solution is flagged as "unphysical". With this in place, the 1.3% non-converging cases could be handled robustly by the computational framework.

5. **Conclusion**

In this work, a heat exchanger modelling framework has been described and demonstrated. The framework addresses the need of models which capture important physical mechanisms and geometrical features of heat exchanger configurations such as tube-in-shell, plate, plate-fin heat exchangers. We have shown how this can be achieved through defining a number of building blocks like fluid and solid elements that are connected by heat nodes through a surface. A possible structure of the framework was illustrated, with examples of how different heat exchanger configurations could be modelled. The proposed solution scheme consisted of alternating between integrating the energy and momentum balances of the fluid elements for each pass with fixed wall temperatures, and solving the wall temperatures with fixed fluid element conditions coming from the fluid calculations. A challenging test case operating similar to the main heat exchanger in a single mixed refrigerant cycle was chosen to validate the robustness of the modelling framework and the solution schemes used. 1000 independent cases with different inlet temperatures, mass flows and pressures selected randomly from a defined range were tested. The cases varied from well balanced heat exchangers to challenging simulations where the heat exchanger was almost at pinch conditions through its whole length. The solution scheme converged in 98.7% of the cases. In the non-converging cases, the mass flow exceeded the physical limits of the heat exchanger. This was handled robustly by temporarily substituting the physical models with a mathematical representation during the iteration scheme.

Acknowledgements

This publication is based on results from the research project "Enabling low emission LNG systems", performed under the Petromaks program. The author(s) acknowledge the project partners; Statoil and GDF SUEZ, and the Research Council of Norway (193062/S60) for support

Nomenclature

Symbols

c_p	Specific heat capacity [J/kg K]
h	Specific enthalpy [J/kg]

This is the accepted version of an article published in Computers and Chemical Engineering
http://dx.doi.org/10.1016/j.compchemeng.2012.10.006

k	Thermal conductivity [W/m K]
x	Direction of the flow [m]
p	Pressure [Pa]
S_i	Perimeter for a surface i [m]
Δx	Length of the fluid element [m]
$\dot{m}$	Mass flow [kg/s]
T	Temperature [K]
dq_i	Heat flow per length for surface i [W]
R	Resistance to heat transfer [Km^2/W]
q_i	Heat flow from surface i [W]
res	Residual [-]
g_i	The residual of the wall temperature iterations [W]
$NS(i)$	Number of surfaces for solid node i [-]
$NKS(i)$	Number of solid bridges for solid node i [-]

Greek letters

α	Heat transfer coefficient [W/m^2 K]
μ	Dynamic viscosity [kg/m^2 s]
ρ	Density [kg/m^3]
σ	Surface tension [N/m]

Subscripts/Superscripts

0	At the inlet of the fluid element
w	Conditions at wall
i	Surface i
F	Conditions in fluid node
f	Frictional flow
g	Due to gravity
l	Liquid phase
v	Vapour phase
tp	Two phase
nb	Nucleate boiling
sat	Saturated conditions
$cond$	Conductive
$conv$	Convective

Abbreviations

This is the accepted version of an article published in Computers and Chemical Engineering
http://dx.doi.org/10.1016/j.compchemeng.2012.10.006

MRHP	Mixed refrigerant, High Pressure
MRLP	Mixed refrigerant, Low Pressure
NG	Natural Gas
VPD	Vertical port distance (for a plate heat exchanger geometry)
HPD	Horizontal port distance (for a plate heat exchanger geometry)

References

Bell, J. K. and M. A. Ghaly. "An approximate generalized design method for multicomponent/partial condensers." AIChE sym s, heat transfer: 1973; 69(72-79).

Bennett, D. L. and J. C. Chen. "Forced convective boiling in vertical tubes for saturated pure components and binary mixtures." AIChE J 1980; 26(3): 454-461.

Boyko, L. D. and G. N. Kruzhilin. "Heat transfer and hydraulic resistance during condensation of steam in a horizontal tube and in a bundle of tubes." Int. J. Heat Mass Tran 1967; 10: 361-373.

Chato, J. C., R. J. Laverman, et al. "Analysis of Parallel Flow, Multi-Stream Heat Exchangers." Int. J. Heat Mass Tran 1971; 14: 1691-1703.

Corberân, J. M., P. F. d. Córdoba, et al. "Semiexplicit Method for Wall Temperaqture Linked Equations (SEWTLE): A General Finite Volume Technique for the Calculation of Complex Heat Exchangers." Numerical Heat Transfer, Part B: Fundamentels 2001; 40(1): 37-59.

Forster, H. K. and N. Zuber. "Dynamics of Vapor Bubble Growth and Boiling Heat Transfer." AIChE Journal 1955; 1: 531-535.

Fredheim, A., O. Jørstad, et al. Coil, a model for simulation of spiral wound LNG heat exchangers. 21st World Gas Conference, Nice.(2000)

Friedel, L. Improved friction pressure drop correlation for horizontal and vertical two phase pipe flow. European Two phase Flow Group Meeting,, Ispra, 5- 8 June.(1979)

Gnielinski, V. "New Equations for Heat and Mass Transfer in Turbulent Pipe and Channel Flow." Int Chem Eng 1976; 16(April): 359-368.

Neeraas, B. O., A. O. Fredheim, et al. "Experimental shell-side heat transfer and pressure drop in gas flow for spiral-wound LNG heat exchanger." Int. J. Heat Mass Tran 2004; 47(2): 353-361.

Paffenbarger, J. (1990). Analysis of Multistream, Plate-Fin Exchangers. Compact Heat Exchangers - A Festschrift dfor A. London. R. K. Shah, A. D. Kraus and D. Metzger, Hemisphere: 727-746.

Pettersen, J., A. Hafner, et al. "Development of Compact Heat Exchangers for CO_2 Air-Conditioning Systems." Int. J Refrig 1998; 21(3): 180-193.

Pingaud, H., J. R. L. Lann, et al. "Steady-State and Dynamic Simulation of Plate Fin Heat Exchangers." Comput Chem Eng 1989; 13(4/5): 577-585.

Powel, M. J. D. A hybrid method for nonlinear equations Gordon and Breach;1988

Prasad, B. S. V. "Fin efficienty and mechanisms of heat exchange through fins in multi-stream plate-fin heat exchangers: development and application of a rating algorithm." Int. J. Heat Mass Tran 1997; 40(18): 4279-4288.

Reneaume, J. M. and N. Niclout. "MINLP Optimization of Plate fin Heat Exchangers." Chem. Biochem. Eng. Q. 2003; 17(1): 65-76.

Schroeder, W., K. Martin, et al. The Visualization Toolkit An Object Oriented Approach to 3D Graphics: Kitware Inc;2006

Selander, W. N. Explicit Formulas for the Computation of Friction Factors in Turbulent Pipe Flow. Chalk River, Ontario CANADA, Chalk River Nuclear Laboratories.1978

Silver, L. "Gas cooling with aqueous condensation." Trans. Inst. Chem. Eng. 1947; 25: 30-47.

Skaugen, G. Simulation of Extended Surface Heat Exchangers using CO_2 as Refrigerant. 4'th IIR-Gustav Lorentzen Conference on Natural Working Fluids, Purdue.(2000)

Skaugen, G. The Effect of Active and Passive Pressure Control - In A Trans-Critical CO_2 Vapour Compresstion Cycle- Part 2 - Simulations and Laborartory Measurements. Thermodynamics, Heat and Mass Transfer of Refrigeration Machines and Heat Pumps - Eurotherm Seminar, Valencia, Spain, IMST.(2003)

Skaugen, G., G. A. Gjøvåg, et al. "Use of sophisticated heat exchanger simulation models for investigation of possible design and operational pitfalls in LNG processes." J. Nat. Gas Sci. Eng. 2010; 2(5): 235-243.

This is the accepted version of an article published in Computers and Chemical Engineering
http://dx.doi.org/10.1016/j.compchemeng.2012.10.006

SLATEC. Common Mathematical Library. Netlib Repository. U. T. Computer Science Dept and O. R. N. Laboratory.1993

This is the accepted version of an article published in Computers and Chemical Engineering
http://dx.doi.org/10.1016/j.compchemeng.2012.10.006